How to build a Maxwell Demon from a 2nd order Phase Change System

Remi Cornwall
Future Energy Research Group
Queen Mary, University of London, Mile End Road, London E1 4NS
http://webspace.qmul.ac.uk/rocornwall or http://vixra.org/author/remi_cornwall

Abstract

This paper presents a summary of research to utilise the massive amount of low grade heat energy, for instance which exists in the worlds oceans, by a new type of magnetic cycle. Developed herein are methods based on 2nd order phase changes that make it possible to irrefutably build a Maxwell Demon. Ferrofluids displaying temporary magnetic remanence are an almost perfect embodiment of the working substance for these cycles. Standard Kinetic Theory, Thermodynamic, Electrodynamic analysis and experiment validates the new cycle.

1. Introduction

Heat energy is energy that has become randomised. Kinetically there is no preferred direction and no preferred direction for potential energy too, as random fields intersect with random orientations. Atomically there is much motion and microscopic energy flux; however in the macroscopic world we live in, the sum of these minute fluxes comes to zero. The concept of high-grade energy degrading to heat is quantitatively expressed by the entropy[1-4] change of a process and dogma states that this must always rise – it is as inevitable as a drop of ink diffusing in a glass of water and not re-concentrating itself back to the original ink drop. Clausius first came up with his integrating factor in the thermodynamic identity with $\delta Q = TdS$ and indentified S, the entropy, as a property of the system which was independent of the path a process took in state space. Boltzmann through advanced classical mechanics[3, 5] realised that entropy was related to the number of states, w, of the system:

$$S = k \ln w \qquad \text{eqn. 1}$$

The entropy was a measure of the statistical spread in measurements of energy, position or momentum of a particle: “high grade” energy (say water at the bottom of a waterfall just before splashing) would have low entropy by there being an observable unidirectional macroscopic flux. After impact, velocity vectors of the ensemble would be randomised; the energy hasn’t disappeared but the entropy had increased.

Maxwell then pondered, after delving into the process of approach to equilibrium distribution of an ensemble, whether the randomising process could be undone by a being[2, 6] able to un-sort the randomness into two reservoirs again and so run a macroscopic heat engine again. Microscopic perpetual motion exists, so what would prohibit macroscopic perpetual motion, given recent interest in the subject and other thermodynamic laws[7, 8]?

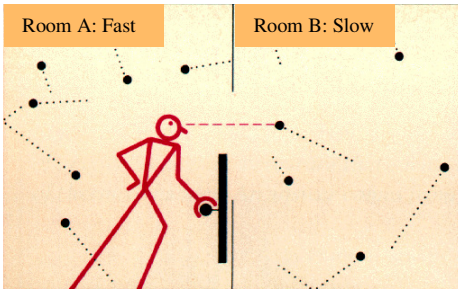

Figure 1 - Maxwell's Demon sorting molecules by speed

Various minds attended to this conundrum in the intervening 75 years or so of debate started by Maxwell and the arguments condensed into three reasons:

- The Demon would be blind in black-body radiation to see anything. Kirchhoff[9].
- A mechanical sorting element of size commensurate to the molecules to effect the sorting, gets randomised too, until ineffective, Smoluchowski[10], Feynman[4] ‘Ratchet and Pawl’.
- Or, to perform sorting would require measurement and expenditure of energy for storage of information, Szilard[11], Brillouin[9], Landauer/Bennett[6].

The last consideration strayed into the area of computing and Information Theory as the first half of the 20th century saw the development of the modern digital computer – this Demon wouldn’t have to be supernatural but a finite state machine with the concomitant use of energy and dissipation to heat. Ironically the very thing it was trying to do, lower entropy, would cause more production of it.

It can be seen that the problem with the Demon is the need to construct something that measures, keeps the processing state of the machinery and then acts, effectively. It is pointless to try and build

anything mechanical; however we shall see that the energy barrier due to material phase, that acts at a microscopic level between molecules, intrinsically measures, "keeps the state of the machinery" and partitions/sorts molecules by kinetic energy. As a quick example of what is meant by this, consider the process of 1st order phase change:

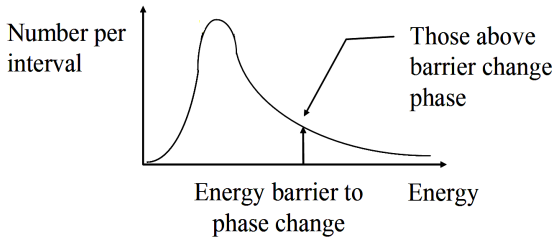

Figure 2 – Unquestionably at least part of a Maxwell's Demon: sorting molecules by speed

As the two phases co-exist, the higher energy phase can be argued to have been "sorted" as an energy barrier was breached by molecules in that phase ("latent heat"). We note that there is no problem, in the Kirchhoff sense, of a measurement being performed above black-body radiation bath as no energy is added to the system to perform the "measurement". Nor is the energy barrier, the sorting element, perturbed by the act of measurement: the barrier is the summation and averaging of potentials from all the molecules, the movement of molecules across it has no change. Finally the maintenance of storage of system state and the finite automaton required to effect the sorting demon is inherent in the machinery of the dynamical equations describing the system. The 1st appendix covers a 1st order phase changing demon but it isn't practical.

Next a 2nd order system was considered based on the order-disorder transition in magnetisation of magnetic materials[1, 12, 13]. Conceptually, magnetic entities small enough to undergo Brownian motion would be aligned by the magnetising field and this requires the input of the magnetising energy:

$$E_{mag} = \int_{M,V} \mu_0 H dM \cdot dV = \mu_0 HMV \qquad \text{eqn. 2}$$

Then the remnant flux would generate electricity by Faraday action and the "dipole-work"([14] appendices 3 and 4):

$$W_{dw} = \int_{M,V} \mu_0 M dM \cdot dV = \frac{1}{2}\mu_0 M^2 V \qquad \text{eqn. 3}$$

This can be made greater than the magnetising energy.

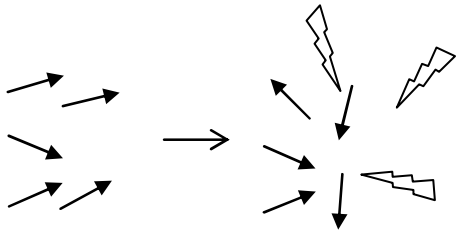

1) Magnetic field orders part of the system.

Energy Input = $\mu_0 HMV$

2) Buffeting from rest of system.

Energy out = $\frac{1}{2}\mu_0 M^2 V$

Figure 3 – A 2nd order Maxwell Demon "Reversed sorting" demon

Unlike the 1st order demon, the 2nd order demon orders a volume first then has the surrounds disrupt it, thus the entropy of the surrounds decrease. This approach has been pursued in depth in the thesis[14][†] and it will be summarised now.

2. Detail on the 2nd order demon

In our research we use a stable nanoscopic suspension of magnetic particles in a carrier fluid called ferrofluid[15]. The particles are so small that they are jostled continuously by the microscopic perpetual motion of heat known as Brownian motion. As a consequence they, on magnetisation display "super-paramagnetism"[13, 15, 16], which on the spectrum from diamagnetism to anti-ferro/ferrimagnetism to paramagnetism to ferri/ferromagnetism, displays properties similar to both paramagnetism and ferri/ferromagnetism: they display no permanent remanence but are somewhat easy to saturate compared to paramagnets due to their large spin moment. Temporary remanence is manifest by two mechanisms:

$$\text{Néel:} \quad \tau_N = \frac{1}{f_0} e^{\frac{KV}{kT}} \qquad \text{eqn. 4}$$

And

$$\text{Brownian:} \quad \tau_B = \frac{3V\eta_0}{kT} \qquad \text{eqn. 5}$$

The first relaxation rate can be understood as internal to the ferrofluid particle and involves lattice vibration and hence it contains the energy term KV related to the crystalline anisotropy constant and the volume of the particle. The latter is related to the jostling of the particle by the suspending fluid and contains an energy term related to the viscosity of the suspending fluid and the volume. Nature uses the principle of least time to determine which dominates the relaxation rate. Obviously these quantities are amenable to engineering.

Another feature they display on rapid magnetic cycling is hysteresis loss[17, 18]. This is most pronounced if the rate of magnetisation is comparable to the relaxation rate. The phenomenon is directly related to the Fluctuation-Dissipation Theorem.[19].

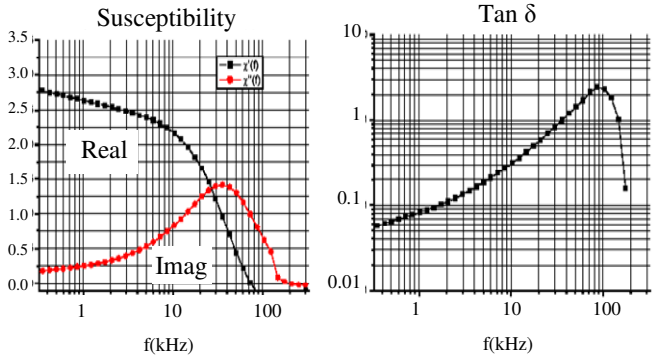

Figure 4 – Hysteresis loss in typical ferrofluid
(Courtesy Sustech Gmbh)
LHS Bodé plot in and out-phase components
RHS: Power loss angle

The cycle (called a micro-cycle) is implemented as a magnetising step followed by a de-magnetising step:

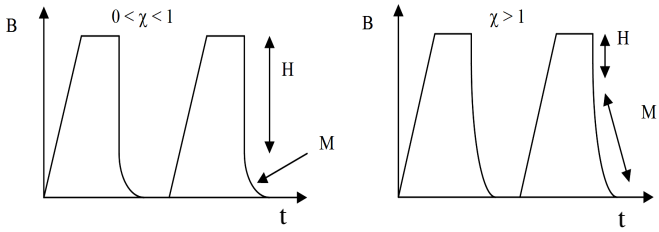

Figure 5 – *Micro-cycle* magnetising pulses for $0 < \chi < 1$ and then $\chi > 1$

The figure above shows a train of magnetising pulses for two cases, small and large susceptibility[13]. Observe how the switch-on phase is slow, so that significant hysteresis loss isn't incurred and the switch-off is abrupt to leave a temporary remnant flux (the "Independent Flux Criterion" sec. 2.3.1). Micro-cycles are completed many times a second and result in an adiabatic cooling of the ferrofluid working substance.

To complete the heat engine, the working substance needs to be placed in contact with an external (albeit only one) reservoir. The plant diagram or macro-cycle is depicted in the next figure. In this figure, the micro-cycles happen many times as the working substance transits the "power extraction area" A-B.

For the purposes of argument, let us dispel concerns about the pressure-volume work that must be expended circulating the fluid against its tendency to be drawn into the magnetised power extraction area by saying there is a portion of the operation when the magnetising fields are switched off and fluid is simply pumped further around to the heat exchange area C-D.

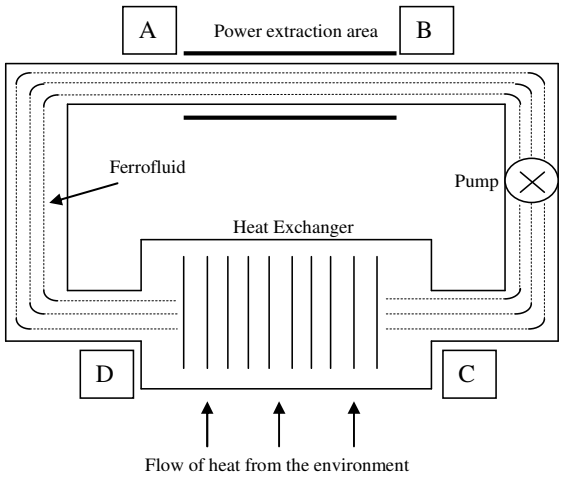

Figure 6 – Plant Diagram (*Macro-cycle*)

We shall develop the theory of the temporary remanence (TR) cycle heat engine by three intersecting analyses: Kinetic Theory, Thermodynamic and Electrodynamic Theories.

2.1 Kinetic Theory

In the thesis[14] a lattice of magnetic dipoles is set up to model the ferrofluid.

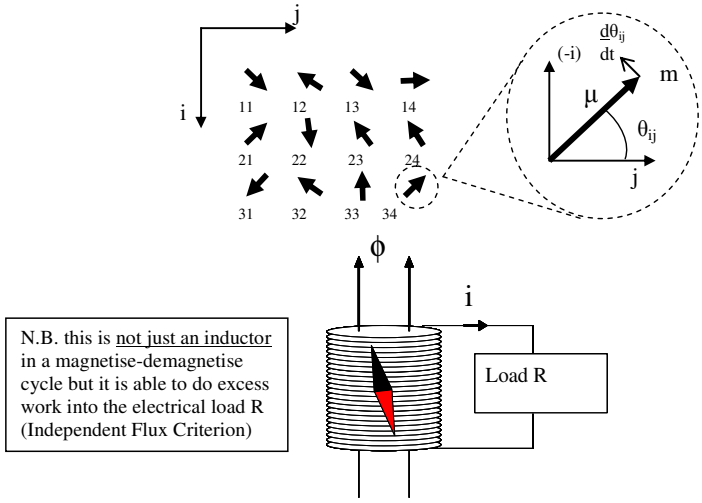

N.B. this is not just an inductor in a magnetise-demagnetise cycle but it is able to do excess work into the electrical load R (Independent Flux Criterion)

Figure 7 – The Kinetic Theory Model

A model of dipole-dipole interactions leads to the angular acceleration of each dipole:

$$\ddot{\theta}_{ij} = \frac{1}{I}\left(-k_{dip} \sum_{\substack{ii=i-1,\\ jj=j-1\\ ii\neq i \wedge jj\neq j}}^{\substack{ii=i+1\\ jj=j+1}} \tau\left(\theta_{i,j}, \theta_{ii,jj}, \mathbf{m}, \mathbf{r}\right) - \mathbf{m}_{ij} \times \mathbf{B}_{ext} \right) \quad \text{eqn. 6}$$

The torque experienced by each dipole is from the external field of the solenoid (B_{ext}) and the dipole-

dipole interactions resulting from the local fields of its neighbours:

$$\tau\left(\theta_{ij},\theta_{ii,jj},\mathbf{m},\mathbf{r}\right)=-\mathbf{m}_{ij}\times\overline{\mathbf{B}_{local.neighbour}} \quad \text{eqn. 7}$$

Taken as a bulk effect, this is of the form const x MdM or the dipole-work[14] (eqn. 3) where $B=\mu_0 M$

The model can be run as a molecular dynamics simulation and the author attempted this to good success, apart from the lack of convergence or *Energy Drift* in these type of simulations from use of non-sympletic algorithms[20]. It wasn't thought worthwhile to pursue this further when, as we shall see, analytical solution exists. Nethertheless the entropies of position and velocity and the temperature are calculated:

$$S_{pos}=const\times\ln\left(\text{standard deviation }\theta_{ij}\right)$$

$$S_{vel}=const\times\ln\left(\text{standard deviation }\dot{\theta}_{ij}\right) \quad \text{eqn. 8}$$

$$T=const\times\text{average}\left(\dot{\theta}_{ij}^2\right)$$

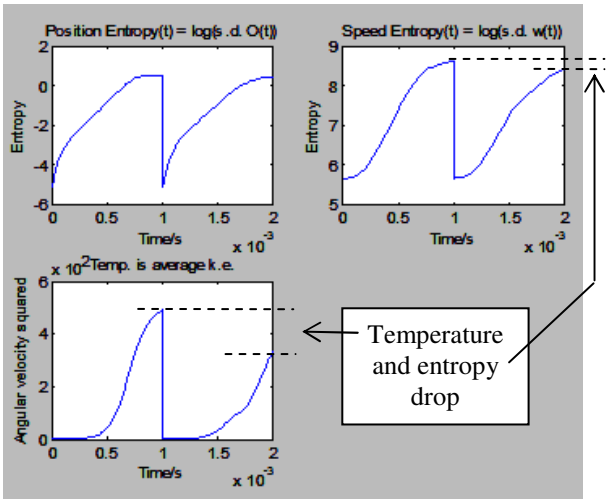

Figure 8 – Relaxing to equilibrium and then the same but with dipole-work

Two simulations were performed, one after the other: In the first simulation the dipoles were all aligned at the start with zero kinetic energy. The simulation shows this "relaxing" to a random orientation (the position entropy increases). The potential energy at the start is converted into random kinetic energy (hence the temperature rises as does the velocity entropy). It is interesting to note that the model randomises itself without any random input. This is just the chaotic dynamics of the 3 (or more) Body Problem[5] – the reason why energy degrades to heat energy.

The second simulation following right after for comparison models relaxation with dipole-work, that is, the assembly generates electrical work which leaves the system and gets dumped into the resistive load.

An analytical solution[14] can be obtained by the statistical averaging of the ensemble eqn. 6:

$$\overline{I\ddot{\theta}_{ij}=-k_v m_{ij}\sum_{ii,jj}\frac{\partial}{\partial t}\left(m_{ii,jj}\cos\theta_{ii,jj}\right)\sin\theta_{ij}}\rightarrow I\ddot{\theta}_{ij}=-k_v\left(m_{ij}\sin\theta_{ij}\right)^2\dot{\theta}_{ij}$$

eqn. 9

Thus each dipole experiences a drag force (hence proportional to the angular velocity $\dot{\theta}_{ij}$) and slows (hence both temperature and entropy decrease) and this is directly related to the dipole-work (eqn. 7). This shows the mechanism for the transduction of heat energy from the working substance to the electrical load.

Kinetic Theory/Statistical Mechanics is the source of the Boltzmann expressions in equations 4 and 5. Anisotropy can be added to the model (eqn. 6) such that rotation cannot occur unless an energy barrier is exceeded. This has the obvious effect of slowing down the relaxation rate. It is shown ([14] section 2.1.3) that compared to the intrinsic anisotropy energy barrier for the ferrofluid, the additional energy barrier from the dipole-work is entirely negligible, thus kinetically the process of the magnetise-demagnetise TR cycle occurs.

2.2 Thermodynamics

The relation between Kinetic Theory, Statistical Mechanics and Thermodynamics is close. The first is a low-level description of single microscopic entities acting in concert; the next is a statistical description of a multitude of these low-level equations; finally thermodynamics relates bulk properties to average properties predicted by Statistical Mechanics.

To be a heat engine, the working substance must first have a property that is a strong function of temperature. This is immediately apparent in equations 4 and 5 with ferrofluid. However with conventional magneto-caloric effect (MCE) engines, focus dwells upon the paramagnetic-ferromagnetic transition and the Curie Point[13, 14]. In the author's thesis a link is made between the TR cycle (figures 5 and 6) and conventional MCE engines by the thermodynamic identity:

$$dU=TdS+\mu_0 Hd\mathcal{M}+\mu_0 Md\mathcal{M} \quad \text{eqn. 10}$$

The last term is the dipole-work such that an amended delta-T equation is derivable by considering 2nd cross-derivatives ([14] section 2.2 and appendix 1) related to the change in magnetising field *and* remnant magnetisation:

$$\Delta T = -\mu_0 \frac{T}{C_H}\left(\frac{\partial \mathcal{M}}{\partial T}\right)_H \left[\Delta H + \Delta M_{rem}\right] \quad \text{eqn. 11}$$

This shows that, unlike conventional MCE cycles the TR cycle can operate below the Curie point (so that ΔT on magnetisation from ΔH is negligible) because the magneto-caloric effect occurs from the new dipole-work term in equation 10. Also we point out that, although ΔT is small, the immense surface area of nanoscopic magnetic particles in contact with the ferrofluid carrier liquid ensures massive heat flow ([14] section 2.2.3).

It is possible to construct ([14] section 2.2.1 to 2.2.4) a temperature-entropy diagram for the micro and macro-cycles.

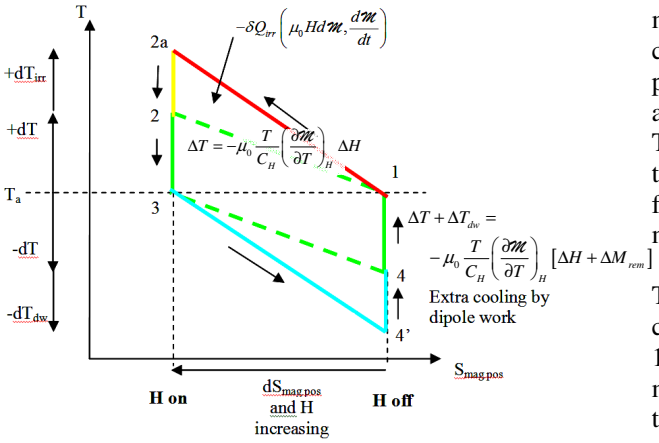

Figure 9 – Temperature- Positional Entropy Diagram for the micro-cycle

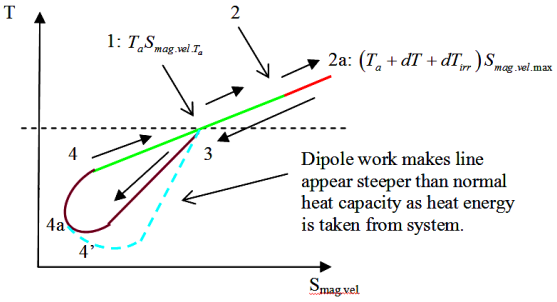

Figure 10 – Temperature- Velocity Entropy Diagram for the micro-cycle

The previous figures depict temperature entropy diagrams for an infinitesimal TR cycle. They are somewhat of an abstraction in that the cycle places the magnetic component of the ferrofluid in contact with the carrier fluid at set points in the cycle (2-3) and (4, 4'-1) and considers them thermally isolated for the rest, whereas in reality the magnetic and fluid systems are always in intimate thermal contact. Thermodynamics requires one to construct a series of states with discernable, stable thermodynamic parameters and this is difficult when the system passes through a series of meta-states.

Figure 9 depicts positional entropy which directly related to magnetic ordering hence the magnetic field of the working substance. The internal cycle represented by numbers 1-4 is the simple MCE in contact with a reservoir. The field switches on between 1 and 2 with the temperature of the working substance raising as the heat capacity is lowered by the magnetising field (the magnetic heat capacity falls and heat is repartitioned to mechanical/kinetic part of the system). Between 2-3 the magnetic system is placed in contact with the ferrofluid carrier liquid which acts as a virtual reservoir and heat is rejected to it. Then between 3-4 the magnetic part, isolated once again, has the magnetising field switched off whereupon the heat capacity rises and heat flows from the mechanical part of the heat capacity to the magnetic part once again such that the magnetic system drops below T_a, the temperature of the carrier fluid. On step 1-4, the magnetic system is placed in contact with the fluid reservoir and heat flows from it to the magnetic system.

The TR cycle is an adjunct to the reversible MCE cycle in contact with an external reservoir at points 1-2a-2, which represents hysteresis heating of the magnetic component and 3-4'-4, which represents the extra cooling by dipole-work.

The step numbers correspond similarly the T-S diagram for the mechanical part of the heat capacity of the magnetic system (fig. 10). We see that it is once again based on the reversible MCE cycle in contact with an external reservoir at steps 1-2-3-4. The difference occurs at point 2-2a with the hysteresis heating (and hence heat transfer between 1-2 on figure 9) and dipole-work cooling 3-4'-4 and heat transfer on figure 9 between 4'-4-1.

One further point is the conversion of the magnetisation energy (eqn. 2) into internal energy as the magnetising field is switched off at point 3-4. This is shown as an extra heat input 3-4a-1 in the diagram below and in figure 10 as steps 3-4'-4a-4-1.

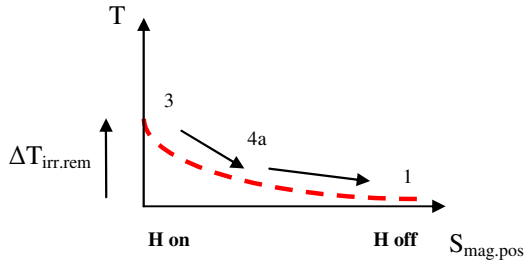

Figure 11 – The magnetising energy becomes internal energy

The consideration of these diagrams([14] appendices 6 and 7) allows the development of the energy balance equation:

$$-C_H \frac{d}{dt}(T_{mechanical}) = \frac{d}{dt}(Q_{external}) - \frac{d}{dt}(W) + \frac{d}{dt}(W_{irreversible}) \quad = 0$$

eqn. 12

This states the obvious really, that the internal energy is dependent on the heat dumped into the ferrofluid minus the dipole-work.

Overall the combined T-S diagram for the positional and mechanical entropies of the working substance is shown in figure 12. Once again, at its core is the reversible MCE cycle 1-2-3-4.

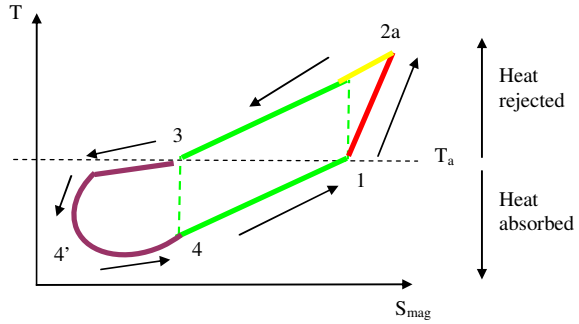

Figure 12 – Temperature-Entropy diagram for the Microcycle Composed of the positional and velocity T-S diagrams sub-cycles

As mentioned in the discussion about the plant diagram (fig. 6), the macro-cycle is made from many concatenated micro-cycles in the power extraction area. The micro-cycles cause the adiabatic cooling (if we neglect hysteresis heat inputs) of the ferrofluid working substance and we arrive at figure 13 (see [14] section 2.2.4 for original figure).

Overall the 2nd order phase change and the dipole-work in the thermodynamic identity make the working substance (eqn. 10) seem like another substance (more of this later in the discussion) with a higher heat capacity. In the lower sub-figure of figure 13 the dipole-work causes a temperature drop ΔT_{DW} for entropy change ΔS as heat energy leaves the system. If we reverse our direction and go up the up trace and imagine we are warming the virtual substance, heat energy not only goes to the working substance but to the external system because of the dipole-work. In comparison the "native" heat capacity of the working substance without the dipole work in lower trace of the sub-figure is:

$$S_0 = C_H \ln(T) + const \qquad \text{eqn. 13}$$

The upper trace has an higher virtual heat capacity:

$$S_{DW} = C_{DW} \ln(T) + const \qquad \text{eqn. 14}$$

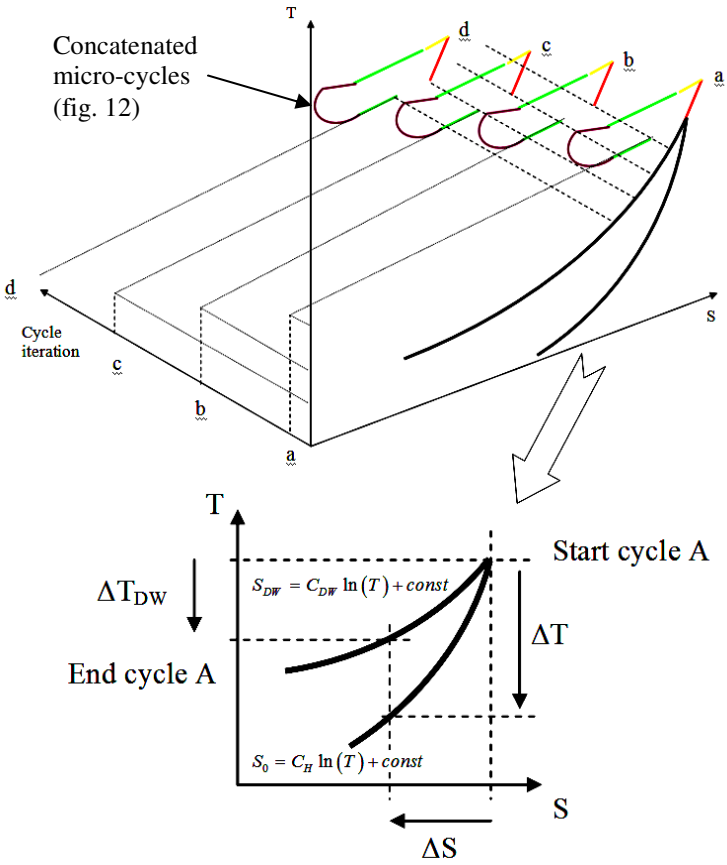

Figure 13 – How Micro-cycles relate to the Macro-cycle on a T-S diagram

Zooming out from the upper sub-figure of figure 13 we arrive at the macro-cycle T-S diagram and then relate that to the plant diagram of figure 6 by the labels A-B-C-D:

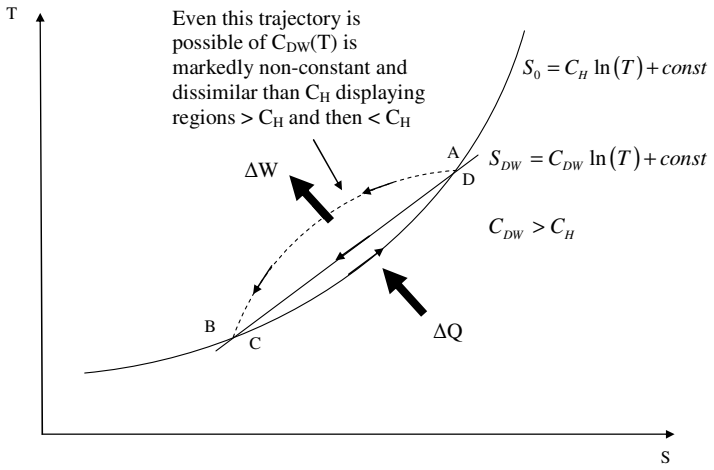

Figure 14 – Macro-cycle T-S diagram related to points on plant diagram

The area between the two trajectories of heat capacity C_H (eqn. 13) and C_{DW} (eqn. 14) is the heat absorbed at the heat exchanger and converted into electrical energy in the power extraction zone.

2.3 Electrodynamics

The Kinetic Theory and Thermodynamic analysis of the previous section have laid the groundwork for the TR cycle. It would seem a simple matter of Faraday/Lenz law collapse of the remnant flux in to a coil attached to an electrical load to deliver the goods of heat energy conversion, as depicted in figure 7. However there is some subtlety in the explanation of the demagnetisation step and a final electrical method to deliver excess power.

2.3.1. Not "just an inductor"

The lower sub-figure in figure 7 and the magnetise-de-magnetise cycle creates the impression that the setup is just a simple electrical circuit and if anything, should act as a dissipative sink of energy due to hysteresis losses. We show that this is not so and that excess electrical energy can enter the circuit from an external source of mechanical "shaft-work", effectively rotating the source of the magnetic flux inside the coil.

Firstly we consider the net electrical work around a magnetisation, de-magnetisation cycle.

$$\oint vi\ dt = -\oint \frac{d\lambda}{dt} i\ dt \qquad \text{eqn. 15}$$

Where λ is the flux linkage. Integrating the RHS by parts:

$$\oint i(t)\frac{d\lambda(t)}{dt}dt = \left[i(t)\lambda(t) - \int \lambda(t)\frac{di(t)}{dt}dt \right]_{0^+}^{0^-}$$

$$= i(0^-)\lambda(0^-) - i(0^+)\lambda(0^+) - F\left(\lambda(0^-), i(0^-)\right) + F\left(\lambda(0^+), i(0^+)\right)$$

eqn. 16

Where F(..) is the integrand of the parts term. Now, since $i(0^+) = i(0^-)$ and $\lambda(0^+) = \lambda(0^-)$ the first two terms cancel. Let a dependent flux be represented by,

$$i(t) \ = \ g\left(\lambda(t)\right) \qquad \text{eqn. 17}$$

Where g is an arbitrary function. The second integral of eqn. 16 can be integrated by parts a second time by applying the chain rule:

$$\int \lambda(t)\frac{di(t)}{dt}dt = \int \lambda(t)\frac{dg\left(\lambda(t)\right)}{d\lambda(t)}\frac{d\lambda(t)}{dt}dt \quad \text{eqn. 18}$$

Thus,

$$\oint \lambda(t)\frac{dg\left(\lambda(t)\right)}{d\lambda(t)}d\lambda(t) = \left[\lambda(t)g\left(\lambda(t)\right) - \int g\left(\lambda(t)\right)\cdot 1\cdot d\lambda(t)\right]_{0^+}^{0^-}$$

$$\Rightarrow G\left(\lambda(0^+)\right) - G\left(\lambda(0^-)\right) = 0$$

eqn. 19

The first term on the RHS cancels due to the flux being the same at the start and end of the cycle. The integrand on the RHS cancels for the same reason. The above result shows that a dependent flux (eqn. 17) cannot lead to net power. The proof sheds more light on the necessary condition for an independent flux*: the flux is constant for any current including zero current* – it bares no relation to the modulations of the current. The proof also dispels any form of dependent relation, non-linear or even a delayed effect. If equation 17 was $i(t) = g\left(\varphi(t-n)\right)$ this could be expanded as a Taylor series about g(ϕ(t)) but there would still be a relation, the flux would still be dependent.

Thus it is a statement of the obvious (the First Law of Thermodynamics) that excess power production in an electrical circuit cannot happen by electrical means alone; flux changes must happen by some outside agency such as electro-mechanical shaft-work to cause energy transduction.

In regard to the Kinetic Theory section and figure 7, we are drawing an analogy with the microscopic dipoles rotating via the randomisation process and the "micro-shaftwork" of heat energy. In fact, considering the energy of a dipole in a field[4, 21, 22]:

$$E = +\mathcal{M}\cdot\mathbf{B} + const \qquad \text{eqn. 20}$$

It matters not whether the magnetic moment is rotated wholesale or randomised between the maximum and minimum energy configuration, it is the same result:

$$\Delta E\big|_{\max}^{\min} = \mathcal{M}B\cos\theta\big|_0^{\pi/2} \text{ or } \mathcal{M}\big|_{\mu_{\max}}^{0} B\cos\theta \quad \text{eqn. 21}$$

2.3.2. Simple resistive load returns less than the input magnetisation energy

We can model the electrodynamics of the de-magnetisation step into a resistive load by a set of state equations[14]:

$$\frac{dM}{dt} = -\frac{1}{\tau}\left(M - \chi\mu_r H\right) \qquad \text{eqn. 22}$$

$$-\frac{d\lambda}{dt} - iR = 0 \qquad \text{eqn. 23}$$

Where,

$$H = \frac{N}{D}i \qquad \text{eqn. 24}$$

And,

$$\lambda = NAB \Rightarrow NA\mu_0\mu_r\left(H + M\right) \qquad \text{eqn. 25}$$

Equation 22 represents very accurately[13, 15, 17, 18] the dynamics of the ferrofluid to a magnetising

field, H‡. The "effective susceptibility" $\chi\mu_r$ is just the product of the susceptibility and the relative permeability of a co-material placed intimately in contact with it. This is just an engineering feature for easier design.

The author then solves the set of equations in the s-domain[14] for the current as R→0:

$$i(t)=\frac{DM_0}{N}e^{-t/\tau'_{ferro}}=\frac{DM_0}{N}e^{-tR/L(1+\mu_r\chi)} \qquad \text{eqn. 26}$$

And calculates the ultimate electrical work delivered to the load $\int_0^\infty i^2(t)Rdt \Rightarrow$

$$W_{dw.L/R\to\infty}=\frac{1}{2}\frac{\mu_0}{(1+\chi\mu_r)}M^2V \qquad \text{eqn. 27}$$

The work done magnetising is given by: $\int HdB\cdot dV$ of which the "H" field energy is discarded, as this can be returned with total efficiency if done by a mechanical magnetisation process or very nearly so with an electronic process ([14] sec. 3.2), leaving:

$$\int_{M,V}\mu_0\mu_r HdM\cdot dV=\mu_0 HM'V$$

The integrand has been resolved with the relative permeability of the material in close proximity to the working substance (the "co-material") subsumed into M'. We can further write the integrand by $M'=\mu_r\chi H$ as (dropping the primes):

$$E_{mag}=\frac{\mu_0}{\chi\mu_r}M^2V \qquad \text{eqn. 28}$$

The dynamical equations can be simulated (or indeed plotted by experiment[14]) and the electrical work plotted against 1/R:

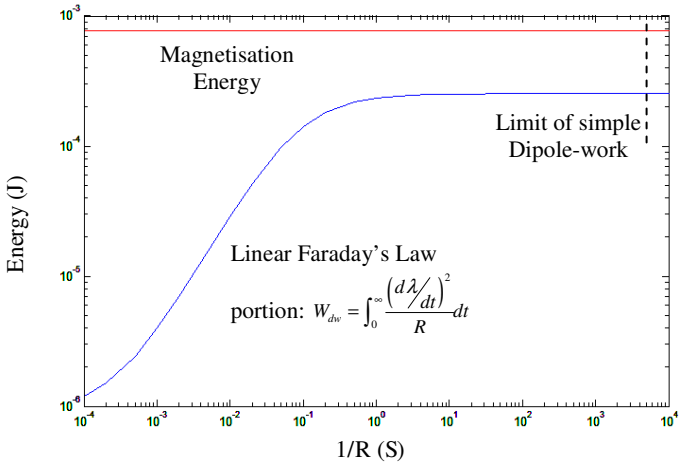

Figure 15 – Magnetisation Energy always exceeds simple dipole-work into resistive load

For the simple arrangement of coil with decaying ferrofluid flux into a resistive load depicted in the lower sub-figure of figure 7, the magnetisation energy input will always exceed the electrical work output. How to circumvent this is discussed in the next section.

2.3.3. The "H-field" cancellation method

The source of the problem for the returned electrical work being less than the magnetisation energy is from the slowing of the current waveforms as the electrical load tends to zero:

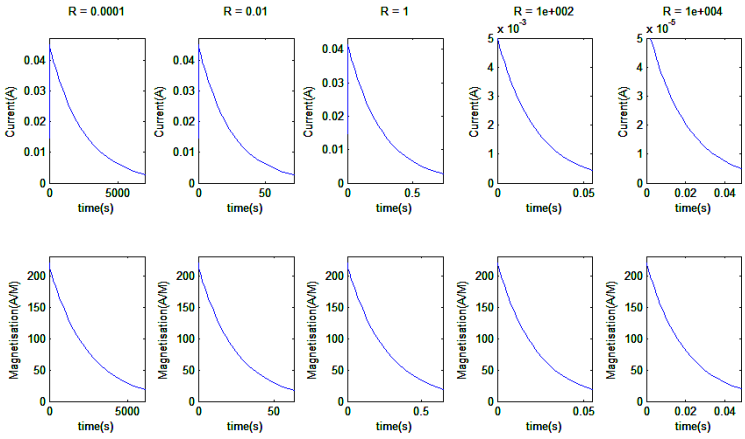

Figure 16 – The slowing current and magnetisation waveforms with lower resistance electrical load

In the s-domain, the current is:

$$I(s)=\frac{\frac{DM_0}{N}}{s^2\tau_{ferro}+s\left(\frac{R}{L}\tau_{ferro}+(1+\mu_r\chi)\right)+\frac{R}{L}} \qquad \text{eqn. 29}$$

The dominant pole of this function shows that the time constant tends to a function purely of the circuit inductance and resistance:

$$s\cong\frac{c}{b}\Rightarrow-\frac{1}{\tau'_{ferro}}=-\frac{1}{\tau_{ferro}+\frac{L(1+\mu_r\chi)}{R}} \qquad \text{eqn. 30}$$

The way around this is to strike out the re-magnetising H-field[4, 12] in equation 22:

$$\frac{dM}{dt}=-\frac{1}{\tau}(M-\chi\mu_r H)$$

Whereupon new current dynamics result:

$$I(s)=\frac{\frac{DM_0}{N}}{s^2\tau_{ferro}+s\frac{R}{L}\tau_{ferro}+\frac{R}{L}} \qquad \text{eqn. 31}$$

The current in the time domain in the limit R→0 is,

$$i(t) = \frac{DM_0}{N} e^{-1/\tau'_{ferro}} = \frac{DM_0}{N} e^{-tR/L} \quad \text{eqn. 32}$$

And then the dipole-work limit by the cancellation method is obtained by $\int_0^\infty i^2(t)\,Rdt$ once again:

$$W_{dw.cancel.L/R\to\infty} = \frac{1}{2}\mu_0 M^2 V \quad \text{eqn. 33}$$

This is seen to be the magnetic field energy of the ferrofluid flux and is greater than the input magnetising energy, equation 28. Simulating the dynamic equations with the approach[14] one can plot and obtain the graph below for one set of parameters $\chi\mu_r \simeq 30$:

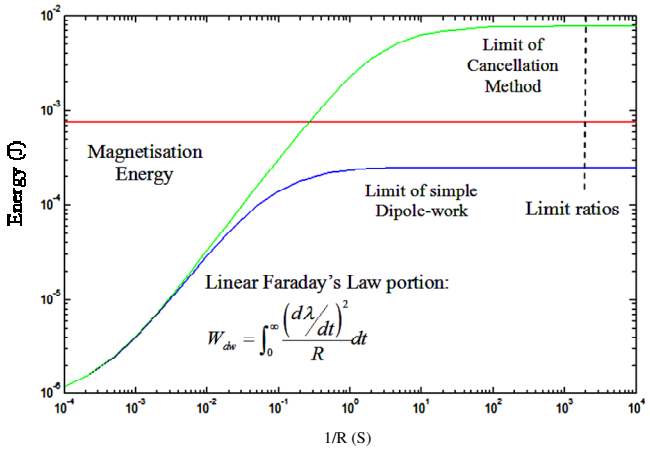

Figure 17 – Dipole-work exceeding magnetisation energy by the H-field cancellation method

We can plot the variation in the limit ratios of the simple dipole-work, the magnetisation energy and the dipole-work with the cancellation method versus parameter $\chi\mu_r$ by taking the ratio of equations 27, 28 and 33:

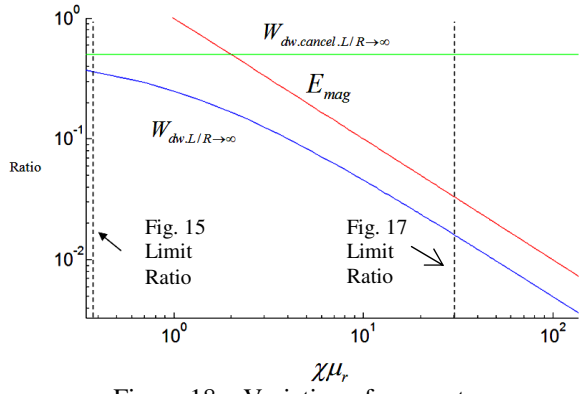

Figure 18 – Variation of parameter $\chi\mu_r$

For all variation of parameters, the magnetisation energy is always greater than the dipole-work without the cancellation method. However if $\chi\mu_r > 2$ the dipole-work, with the cancellation method, will exceed the magnetisation energy input. The power produced by the device is then:

$$P = \left(W_{dw.cancel} - E_{mag} - W_{losses}\right) F_{cycle}$$

Confirming what was said in the thermodynamic section and equation 12.

The circuit to perform the cancellation method is shown below and detailed description of its mechanism of action can be found in the thesis ([14], sec. 4.3).

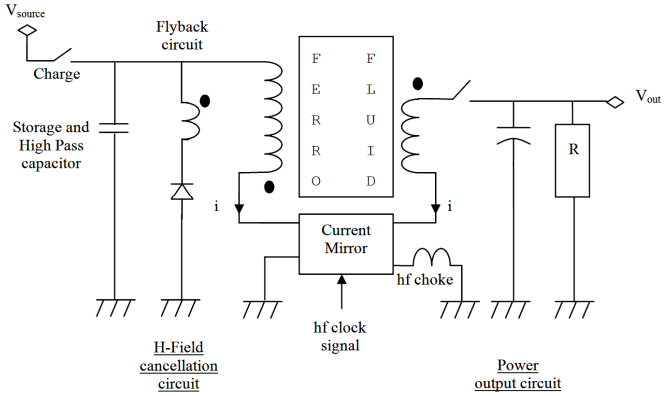

Figure 19 – The H-Field Cancellation Scheme (LHS circuit)

The circuit works by sampling the current in the power circuit (RHS) and makes a "chopped" proportional copy of it.

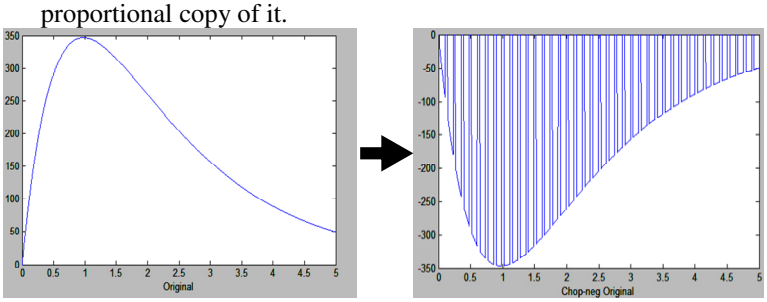

Figure 20 – Sampling, inverting and "chopping" the current/H-field

The LHS then generates its own H-field which sums with the RHS. The ferrofluid naturally low-pass filters this resultant H-field because of its high harmonics and even more so at very high frequency where the ferrofluid will not exhibit a response nor dissipation (fig. 4). One can observe how the resulting H-field is reduced in the rightmost figure.

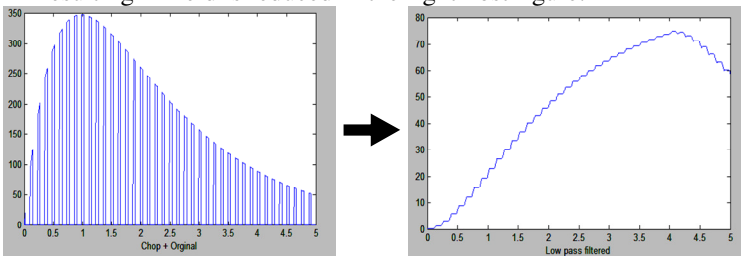

Figure 21 – The resultant high frequency H-field gets low-pass filtered

Even better cancellation comes from asymmetric summation of the inverted, chopped field to the magnetising field. Below is shown the result of summing -1.5 x the original field:

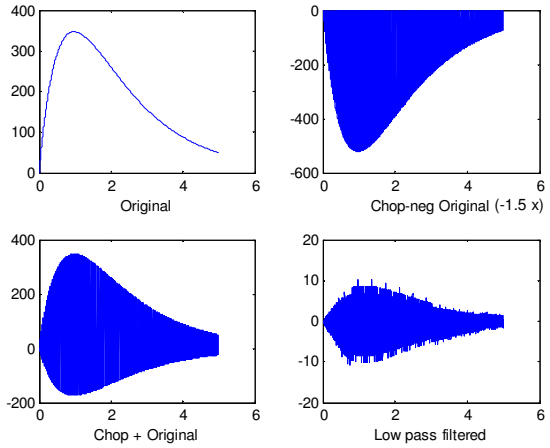

Figure 22 – Asymmetric sampling and summation

The author analyses the electrical work required to operate the H-field cancellation scheme ([14], sec. 4.3.1) and notes that by the inclusion of filtering elements and the "flyback" circuitry, that the LHS circuit only does work establishing the cancellation field and this can be done with high efficiency in a regenerative manner.

3. Discussion

We have a system via standard analysis (both Kinetic Theory and Thermodynamics) and experiment that is permissible, yet violates the Kelvin-Planck form of the 2nd Law by forming a virtual cold reservoir in its operation (figs. 6, 12 and 14). The introduction showed that counter to the anti-Maxwell Demon arguments, physical systems *unquestionably already exist* that do part of the sorting process without special measures (fig. 2). The stretch to 2nd order processes and the reverse-sorting procedure (fig. 3) by the electrical methods already discussed is not that hard a leap.

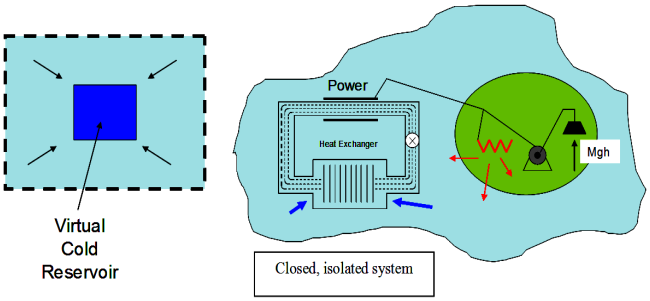

Figure 23 – A Thermodynamic Paradox – macroscopic work at constant entropy

3.1 The Arrow of Time

The Second Law of Thermodynamics implies that there is a preferred direction of time but this is in conflict with the underlying equations of motion that are time reversible[5] or even the equilibrium state where dS = 0. The Boltzmann H-Theorem[19] can be seen to be using circular logic: starting from the premise that the particles are statistically uncorrelated (i.e. at maximum entropy) it derives a quantity resembling entropy that increased with time. This seemed satisfying. The true reason came from Chaotic Dynamics[23-25] which was initiated by the new semi-quantitative methods of Poincaré in his investigation of celestial mechanics.

It had been known for sometime that there was no general solution of the three-body problem[5] and modern Dynamic Systems Theory has shown by 'toy' models such as the Smale Horseshoe or Henon iterative maps, that distil the essence of complex dynamic systems, that points close in phase space will diverge exponentially (the so called Lyapunov exponent) leading to the churning of paths in a bounded chaotic attractor and the Ergodic Theorem (hence bounded and not violating the 1st Law). The system state vector in a short time accrues inaccuracy with exponential divergence and herein is the Arrow of Time.

3.2 The Thermodynamic Mechanism for a Maxwell Demon

Should we be so scared by the concept of type 2 perpetual motion? We already know that heat energy *is* microscopic perpetual motion with the continual exchange of kinetic to potential energy; two-body simple harmonic oscillation does this and we might extend the notion and call it "n-body complicated oscillation". Clearly our Maxwell Demon is part of the n-body complicated oscillatory dynamics of the system and we should find the law, mechanism or rationale providing the underlying reason why this is possible.

If one deals with microscopic fluxes at equilibrium, one can say that an exceedingly large amount of *microscopic work* can occur at *constant temperature,* as this clearly is how individual particles rise in potential at equilibrium. There is no conflict with the Carnot result if one takes this viewpoint, that as $T_H - T_C \rightarrow 0$, the efficiency η tends to zero,

$$\frac{\Delta W}{\Delta Q_H} = \eta = \left(\frac{T_H - T_C}{T_H} \right)$$

We argue that the microscopic work-flows at constant temperature become essentially limitless based on the microscopic heat-flows, which are essentially limitless too. All we are saying is that if the micro-flow of heat, δQ is exceedingly large near (or approaching near) constant temperature,

then even if η is not quite zero, the work-flows will be large like the microscopic heat-flows too. This is guaranteed by the statistical fluctuation of temperature at equilibrium[3, 19], figure 24.

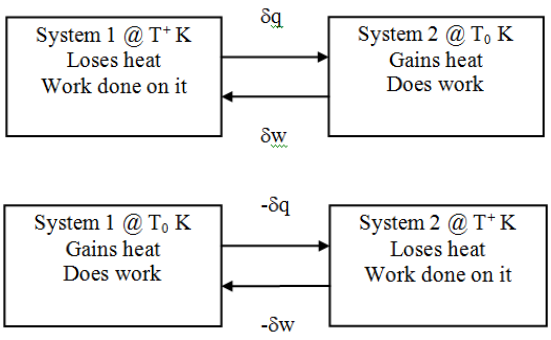

Figure 24 – Statistical fluctuation in temperature with micro-heat and micro-work flows

We are now in a position to see why phase change is key to making a Maxwell Demon. At equilibrium between two phases, microscopic fluctuations in temperature effectively form microscopic heat engines that are able to do work against the phase boundary. As has already been pointed out, figure 2 is already able to form part of a demon and sort molecules without extra energy input because:

Constant Temperature Theorem

At constant temperature microscopic heat and work are available and can partition energy across a phase boundary.

So if a *microscopic* demon is possible how is a *macroscopic* demon made?

Phase Transition Sorting Theorem

Macroscopic work is obtainable from microscopic work processes at constant temperature by the working substance undergoing a phase transition.

By definition, a phase is a macroscopic representation of underlying microscopic properties. In a sense, the phase change has "magnified" the microscopic demon.

This can be understood from the thermodynamic identity:

$$dU = TdS - PdV + \mu(P,T,\varphi)$$

Where ϕ is a potential function of position.

Since dU is an exact integral, any means of cycling the working substance by any of the variables of the system will not produce excess energy from the lowering of the internal energy of the working substance. Let us understand this more by reviewing a conventional Carnot engine.

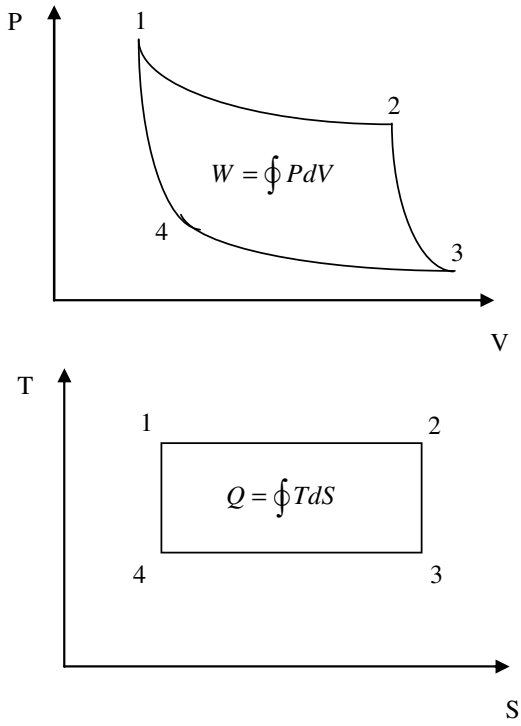

Figure 25 – PV and TS diagrams for Carnot Engine

The working substance being only one material is constrained to traverse fixed trajectories in PV or TS space. The familiar alternating of isothermals with adiabatics is required to map out an area, as moving reversibly along 1-2: isothermal-adiabatic or 1-2-3: isothermal-adiabatic-isothermal, will not return to the starting co-ordinates. The last step maps out an area so that:

$$\Delta U = \Delta Q - \Delta W = 0$$

$$\Rightarrow \Delta W = \Delta Q$$

This cannot be done with just one reservoir and the last step 3-4 must come into contact with the lower reservoir.

Consider now the meaning of the chemical potential, it is the thermodynamic potential per particle:

$$du = Tds - pdV + \mu \qquad \text{eqn. 34}$$

Lower case indicates that this is per particle. The chemical potential has two parts, the internal and external[1]. If at some point in a thermodynamic cycle an external potential μ_{ext} is added or changed then the thermodynamic identity can be made inexact,

$$\delta u = Tds - pdV + \mu_{\text{int}} + \mu_{ext} \qquad \text{eqn. 35}$$

A change of μ by external potential can only correspond to a phase change as this will introduce potential energy terms, such as that pertaining to latent heat or new magnetisation energy terms, for instance i.e. dipole-work (eqn. 10). It is as though we have a different working substance not constrained to the trajectories of one substance in PV or TS space and we can achieve net work from only one reservoir. For instance, in the hypothetical PV diagram shown below, the working substance might expand adiabatically from 1-2, undergo a phase change (by some agency, appendix 1) and do work 2-3 and then be placed back in contact with the one reservoir 3-1.

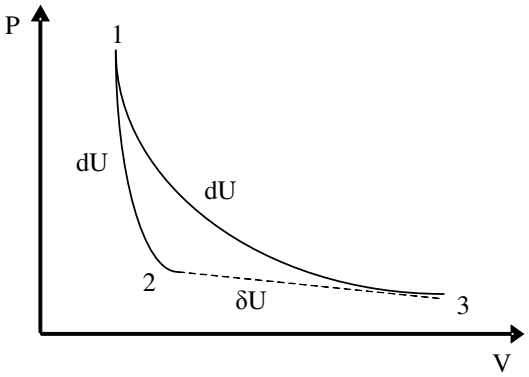

Figure 26 – Illustrative PV diagram

These considerations are not unlike the TS diagrams in figures 12 and 14.

4. Conclusion

This paper is built on the foundations of Kinetic Theory, Thermodynamics, Electrodynamics and experiment.

Kinetic Theory shows that the relaxing magnetic field acts as a velocity damping term to each magnetic particle undergoing Brownian motion. The electromagnetic field couples to the thermal system, the electromagnetic system then couples to the external electrical system to which power is transferred.

Thermodynamics shows:

- A "delta T", a change in temperature of the working substance from the magnetic work related to the magnetic properties of the material.
- On considering the magnetic enthalpy[14], a new term "MdM" called the dipole-work is added onto the thermodynamic identity and is only relevant when heat transfer occurs. This happens on the second half of the Temporary Remanence cycle. This ties in with the Kinetic Theory where MdM is the velocity damping term.
- T-S diagrams show how the entropies of the magnetic system form a heat engine. Tying in with Kinetic Theory, once again, the variation in entropy associated with the velocity distribution of the magnetic particles is the source of the heat transference.
- An energy balance equation that shows how the internal energy of the working substance falls with electrical work it performs.

Electrodynamics shows:

- The dynamics of the electrical generation process.
- The work delivered to an electrical load by Faraday/Lenz/Maxwell induction law and that this is of the form MdM, once again.
- The work delivered to an electrical load with the field cancellation technique and that this exceeds the input magnetisation energy substantially. The difference comes from the conversion of heat energy to electrical energy.

It is possible to obtain work from only one thermodynamic reservoir.

Appendix: 1st order phase change demon

Originally a column with an hygroscopic solution was envisioned where the head of water condensed at height would be sufficient to force water out of a reverse osmosis membrane. This setup was meant to make a "phase changing catalyst" which would reside in a closed, isolated system (with gravity) containing water in the liquid and vapour phases.

The analysis is tedious but we learn that the column would be several kilometres high (thought there is still enough vapour pressure to drive into solution at the top of the column). However flow losses would realistically result in a trickle of water at the base.

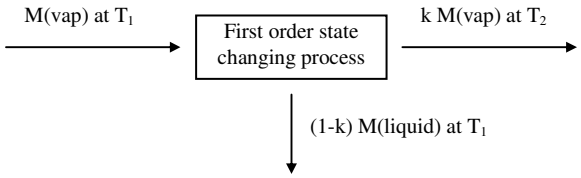

A Phase Changing 'Catalyst'

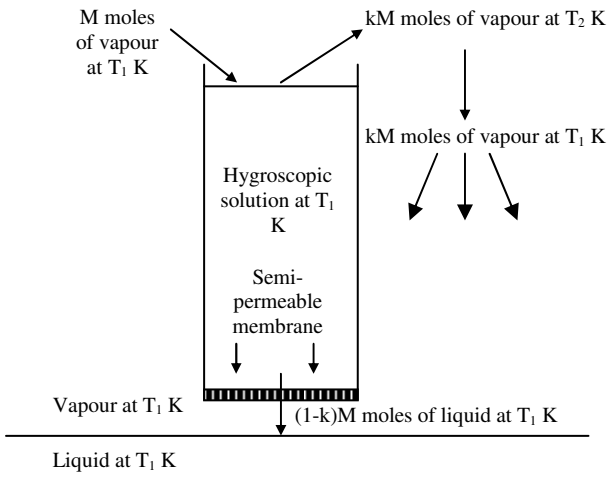

Figure 27a,b – Hygroscopic "phase changing catalyst" column demon

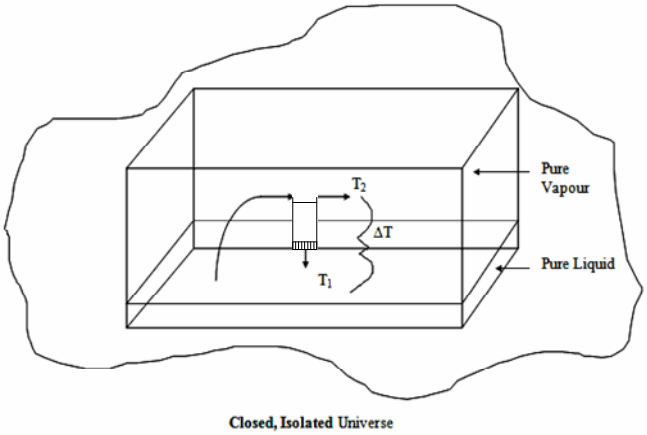

Figure 28 – Device in two phase system

References

1. Kittel C., K.H., *Thermal Physics*. W. H. Freeman and Company, San Francisco. Vol. 2nd ed. 1980.
2. Maxwell, J.C., *Theory of Heat*. Longmans, Green and Co., London Vol. Chap. 12. 1871.
3. Landau, L., *A Course in Theoretical Physics: Statistical Physics*. Vol. Vol. 5. 1996: Butterworth Heinemann.
4. Feynman, L., Sands, *The Feynman Lectures on Physics*. Addison-Wesley, Reading, Massachusetts. Vol. Vol.1, Vol. 2 1989. 14.7, 15.1-6, 35.4
5. Landau, L., *A Course in Theoretical Physics: Mechanics*. Vol. Vol. 1. 1982: Butterworth Heinemann.
6. Harvey L. S., A.F.R., *Maxwell's Demon: Entropy, Information and Computing*. Adam Hilger, Bristol 1991.
7. Santhanam, P., D.J. Gray, and R.J. Ram, *Thermoelectrically Pumped Light-Emitting Diodes Operating above Unity Efficiency*. Physical Review Letters, 2012. **108**(9): p. 097403.
8. Kolář, M., et al., *Quantum Bath Refrigeration towards Absolute Zero: Challenging the Unattainability Principle.* Physical Review Letters, 2012. **109**(9): p. 090601.
9. Brillouin, L., *Science and Information Theory*. Academic Press Inc., New York 1956. Chaps. 13, 14.
10. Smoluchowski, M., *Experimentell nachweisbare, der Ublichen Thermodynamik widersprechende Molekularphenomene.* Phys. Zeitshur., 1912. **13**.
11. Szilard, L., *On the Decrease of Entropy in a Thermodynamic System by the Intervention of Intelligent Beings.* Physik Z., 1929. **53**: p. 840-856
12. Bozorth, R.M., *Ferromagnetism*. IEEE Press 1978.

13. Aharoni, A., *Introduction to the Theory of Ferromagnetism*. Oxford Science Publications 1996.

14. Cornwall R. O., *Novel Thermodynamic Cycles involving Ferrofluids displaying Temporary Magnetic Remanence.* http://webspace.qmul.ac.uk/rocornwall/, 2013. http://vixra.org/abs/1311.0078

15. Rosensweig, R.E., *Ferrohydrodynamics*. Cambridge University Press. 1998.

16. Vallejo-Fernandez, O'Grady, Patel, *Mechanisms of hyperthermia in magnetic nanoparticles.* J. Phys. D: Appl. Phys., 2013. **46**.

17. Fannin, P.C., *A Study of the Complex Susceptibility of Ferrofluids and Rotational Brownian Motion.* Journal of Magnetism and Magnetic Materials, 1987. **65**: p. 279-281

18. Fannin, P.C., *On the Analysis of Complex Susceptibility Data of Ferrofluids.* Journal of Physics D: Applied Physics, 1988. **21**: p. 1035-1036

19. Landau, L., *A Course in Theoretical Physics: Kinetics*. Vol. Vol. 10. 1981: Butterworth-Heinemann.

20. Haile J. M., *Molecular Dynamics Simulation*. 1997: John Wiley and Sons.

21. Jackson, J.D., *Classical Electrodynamics*. 2nd ed. 1975: Wiley.

22. Landau, L., *A Course in Theoretical Physics: Classical Theory of Fields*. Vol. Vol. 2 1982: Butterworth-Heinemann.

23. *The Ergodic Theorem*, in *Encyclopaedia Britannica Inc.*

24. Jordan D. W., S.P., *Nonlinear Ordinary Differential Equations*. Clarendon Press Oxford. Vol. 2nd ed. . 1991.

25. Kapitaniak, T., *Chaos for Engineers*. Springer 1998.

[‡] Feynman in his lecture notes is quite scathing about the term "H-field" which is used by electrical engineers and those working in the magnetics of materials,

> "… there is only ever B-field, the magnetic field density … it is a mathematical arrangement to make the equations of magneto-statics come out like electro-statics when we know isolated magnetic poles don't exist by Maxwell's Equations, div B = 0."